Received 7 June 2023
Revised 15 August 2023
25 October 2023
Accepted 27 November 2023

Effect of climate change on reference evapotranspiration at the subnational scale: case study of Egypt

Abdelhamid Ads
Indian Institute of Technology Roorkee, Roorkee, India
Santosh Murlidhar Pingale
National Institute of Hydrology, Roorkee, India, and
Deepak Khare
Indian Institute of Technology Roorkee, Roorkee, India

Abstract

Purpose – This study's fundamental objective is to assess climate change impact on reference evapotranspiration (ET_o) patterns in Egypt under the latest shared socioeconomic pathways (SSPs) of climate change scenarios. Additionally, the study considered the change in the future solar radiation and actual vapor pressure and predicted them from historical data, as these factors significantly impact changes in the ET_o.

Design/methodology/approach – The study utilizes data from the Coupled Model Intercomparison Project Phase 6 (CMIP6) models to analyze reference ET_o. Six models are used, and an ArcGIS tool is created to calculate the monthly average ET_o for historical and future periods. The tool considers changes in actual vapor pressure and solar radiation, which are the primary factors influencing ET_o.

Findings – The research reveals that monthly reference ET_o in Egypt follows a distinct pattern, with the highest values concentrated in the southern region during summer and the lowest values in the northern part during winter. This disparity is primarily driven by mean air temperature, which is significantly higher in the southern areas. Looking ahead to the near future (2020–2040), the data shows that Aswan, in the south, continues to have the highest annual ET_o, while Kafr ash Shaykh, in the north, maintains the lowest. This pattern remains consistent in the subsequent period (2040–2060). Additionally, the study identifies variations in ET_o, with the most significant variability occurring in Shamal Sina under the SSP585 scenario and the least variability in Aswan under the SSP370 scenario for the 2020–2040 time frame.

Originality/value – This study's originality lies in its focused analysis of climate change effects on ET_o, incorporating crucial factors like actual vapor pressure and solar radiation. Its significance becomes evident as it projects ET_o patterns into the near and distant future, providing indispensable insights for long-term planning and tailored adaptation strategies. As a result, this research serves as a valuable resource for policymakers and researchers in need of in-depth, region-specific climate change impact assessments.

Keywords Reference evapotranspiration (ET_o), Climate change, CMIP6,
Shared socioeconomic pathway scenarios (SSP_s), Penman–Monteith method, Egypt

Paper type Research paper

The authors appreciated worldClim.org for providing free access to climate change model data.

ArcGIS toolbox: To access the ArcGIS toolbox developed at the study, contact abdelhamedads@gmail.com

Arab Gulf Journal of Scientific Research
Vol. 42 No. 4, 2024
pp. 1736-1754
Emerald Publishing Limited
e-ISSN: 2536-0051
p-ISSN: 1985-9899
DOI 10.1108/AGJSR-06-2023-0234

1. Introduction

The world is currently facing a significant challenge of climate change caused by human activities, as greenhouse gas emissions are at an all-time high. Climate change has a wide-ranging impact on both human and natural systems. The atmosphere has warmed, and sea levels have risen as a result of melting ice sheets (IPCC, 2014). Different regions of the world are affected differently by global warming, and the Mediterranean region is one of the primary hot spots for climate change due to the expected changes in temperature and rainfall (Giorgi, 2006). Studies have shown that climate change is accelerating in developing countries, particularly in the Middle East and North African (MENA) region (Zakaria, Al-Ansari, & Knutsson, 2013). Egypt is particularly vulnerable to climate change due to its high population growth and large population living in a narrow area around the Nile River (Affairs, 2018).

Scenarios play a critical role in any research and assessment of climate change. They depict the different potential futures given fundamental uncertainties and help predict the long-term consequences of current or near-term decisions (IPCC, 1992). Various scenarios have been developed in the past, such as the special report on emissions scenarios (SRES) (A1, A2, B1 and B2) and the representative concentration pathways (RCPs) (RCP 2.6, RCP 4.5, RCP 6 and RCP 8.5) (Moss *et al.*, 2008). The most recent scenarios are the shared socioeconomic pathways (SSPs), which were utilized in the Intergovernmental Panel on Climate Change (IPCC) sixth assessment report, published in 2020–2021. The SSPs integrate the analysis of future climate impacts, vulnerabilities, mitigation and adaptation. They describe different socioeconomic developments such as sustainable development, regional rivalry, inequality, fossil-fueled development and middle-of-the-road development (SSP1, SSP2, SSP3, SSP4 and SSP5) (Riahi *et al.*, 2017). The SSP scenarios have been previously employed in research conducted in Egypt, particularly in the investigation of the impacts of climate change on water resources (Hamed & Shahid, 2022; Nashwan & Shahid, 2022).

Reference evapotranspiration (ET_o) is defined as "the rate of evapotranspiration from a hypothetical reference crop with an assumed crop height of 0.12 m, a fixed surface resistance of 70 sm^{-1}, and an albedo of 0.23 (Allen, Pereira, Raes, & Smith, 1998). ET_o is one of the primary factors in the hydrological cycle, as 65% ± 26% of global evaporation happens on the soil surface, not the water surface (Good, Noone, & Bowen, 2015). The ET_o is a hydrological variable that is particularly sensitive to climate change (Bao *et al.*, 2012), highlighting the importance of studying the effects of climate change on ET_o. ET_o is a key factor in many vulnerability studies on climate change and its impact on water resources availability, irrigation water requirements, agriculture and other related fields (Cardona *et al.*, 2012). ET_o exhibits positive sensitivity to all the climate variables except relative humidity (Zhang, Chen, & Paw U, 2019). Among these variables, mean air temperature is the primary factor that influences changes in ET_o, followed by relative humidity, sunshine hours and wind speed (Liu, Zhang, & Li, 2014; Sun *et al.*, 2020).

Several studies were carried out previously to find climate change's impact on ET_o. These studies demonstrated that ET_o varies with climatic conditions and regions (Das, Datta, Sharma, & Goswami, 2022; Gurara, Jilo, & Tolche, 2021; Liu, Li, Zhao, & Han, 2020; Rim, 2009; Tadese, Kumar, & Koech, 2020). For instance, in Ningxia, Zhao *et al.* (2020) investigated the effects of climatic changes on reference crop ET_o across various climatic zones, revealing notable increases in ET_o. In two more studies conducted in Thailand (Arunrat *et al.*, 2020, 2022), researchers investigated the impact of climate change on crop yields under various scenarios, including the RCPs and SSPs. They identified a significant decrease in crop yields. In Egypt, previous studies have shown that ET_o is expected to increase significantly in the 2050s and 2100s, compared to current levels, under climate change scenarios A1, A2, B1 and B2 (Farag, Abdrabbo, & Ahmed, 2014). Another study, which analyzed data from the four RCP scenarios (RCP2.6, RCP4.5, RCP6.0 and RCP8.5) for the three-time series (2011–2040, 2041–2070 and 2071–2100), also found that ET_o would increase significantly (Abdrabbo, Farag, & El-Desokey, 2015).

The study objective is to address the gaps on use of conventional climate data, including parameters such as radiation, relative humidity and wind speed. In contrast, this study uniquely focuses on investigating the impact of actual vapor pressure and solar radiation variations, acknowledging their substantial influence on the dynamics of ET_o. Furthermore, while previous investigations were based on older climate change scenarios, this study is dedicated to exploring the most up-to-date scenarios, known as SSPs. The study's central aim is to assess the effects of climate change on ET_o at a subnational scale, thereby providing valuable insights for decision-makers in selecting appropriate adaptation strategies. To achieve the objectives, we utilized the Penman–Monteith method for calculating ET_o, a method whose effectiveness in accurately estimating ET_o across a range of agroclimatic regions within Egypt has been consistently demonstrated (Allen *et al.*, 1998; El Afandi and Abdrabbo, 2015). In addition, statistical methods were employed to project future solar radiation and actual vapor pressure based on historical data, acknowledging their substantial influence on ET_o changes, an aspect overlooked in previous studies. Furthermore, we utilized climate data from the Coupled Model Intercomparison Project Phase 6 (CMIP6) models under the SSP climate change scenarios.

2. Data and method

2.1 Study area

Egypt has a total area of about one million km^2 and is located in the African continent's northeastern corner (Figure 1). Hot and dry summers and mild winters characterize Egypt's climate, where rainfall is deficient, irregular and unpredictable. Most of Egypt's land is desert,

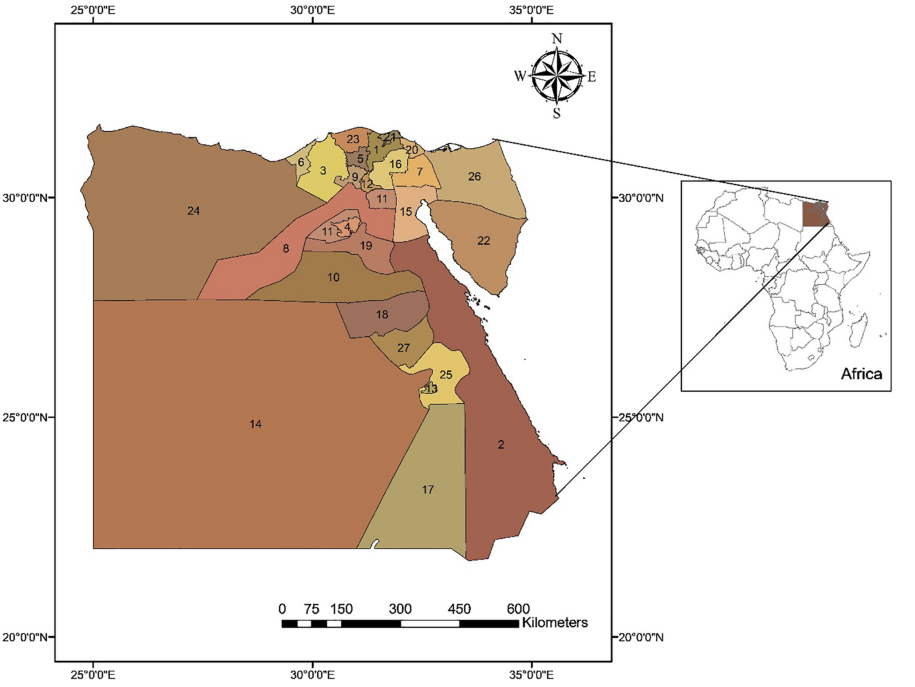

Figure 1.
The study area

Source(s): Credited to the authors

and 3% of the agricultural area is around the Nile River. The Nile River is the main source of irrigation, with an annual allocated flow of 55.5 km^3/year. Egypt is one of the countries under water scarcity. The currently available water resources are 55.5, 1.6 and 2.4 Billion Cubic Meter per year (BCM/yr) from the Nile River, actual rainfall on the northern Mediterranean Sea and groundwater, respectively. The total water supply is 59.5 BCM/yr. However, the total water requirement for different sectors is 79.5 BCM/yr. Hence, the water needs and availability gap is about 20 BCM/yr (MWRI, 2014). The agricultural process, involving water utilization across diverse facets of crop cultivation, including irrigation and accounting for water losses during transportation and the irrigation process, stands as the predominant consumer of water in Egypt. This sector commands a substantial portion, exceeding 85% of the total water demand (Planning Sector, 2005). Egypt has 27 governorates (subnational scale), four of them without significant agricultural areas: 14, 22, 23 and 26 (CAPMAS, 2021) (Table 1).

2.2 Data used

The data used in this study is monthly historical and future climate data at 2.5 min of spatial resolution. In terms of the historical climate data, the data is the WorldClim version 2.1 climate data for 1970–2000, which was published in January 2020 (Fick *et al.*, 2017). The data are minimum, mean and maximum temperature (°C), solar radiation (kJ m^{-2} day^{-1}), wind speed (m s^{-1}) and water vapor pressure (kPa).

For future climate data, the data is the output of the models of the CMIP6 (Table 2). Downscaled and bias-corrected data were downloaded for four SSP scenarios (SSP126, SSP245, SSP370 and SSP585) (Meinshausen *et al.*, 2020; Moss *et al.*, 2010) for six models. The data is a monthly minimum and maximum temperature over 20 years (2021–2040 and 2041–2060) at 2.5 min of spatial resolution.

The six models used in this study are BCC-CSM2-MR (Wu *et al.*, 2019), CanESM5 (Swart *et al.*, 2019), CNRM-CM6-1 (Voldoire *et al.*, 2019), IPSL-CM6A-LR (Boucher *et al.*, 2020), MIROC-ES2L (Hajima *et al.*, 2020) and MRI-ESM2-0 (Yukimoto *et al.*, 2019). These models were chosen based on their accessibility at no cost. Additionally, we aimed to incorporate models from diverse geographical regions to ensure a comprehensive representation (Table 2).

No.	Name	No.	Name
1	Ad Daqahliyah	15	As Suways
2	Al Bahr al Ahmar	16	Ash Sharqiyah
3	Al Buhayrah	17	Aswan
4	Al Fayyum	18	Asyut
5	Al Gharbiyah	19	Bani Suwayf
6	Al Iskandariyah	20	Bur Sa`id
7	Al Isma`iliyah	21	Dumyat
8	Al Jizah	22	Janub Sina'
9	Al Minufiyah	23	Kafr ash Shaykh
10	Al Minya	24	Matrouh
11	Al Qahirah	25	Qina
12	Al Qalyubiyah	26	Shamal Sina'
13	Al Uqsur	27	Suhaj
14	Al Wadi al Jadid		

Source(s): Credited to the authors

Table 1.
Egypts' governorates

Model	Institute	Country
BCC-CSM2-MR	Beijing Climate Center	China
CanESM5	Canadian Center for Climate Modeling and Analysis	Canda
CNRM-CM6-1	Center National de Recherches Météorologiques	France
IPSL-CM6A-LR	Institut Pierre-Simon Laplace	France
MIROC-ES2L	The University of Tokyo, National Institute for Environmental Studies, Japan Agency for Marine-Earth Science and Technology	Japan
MRI-ESM2-0	Meteorological Research Institute	Japan

Source(s): Credited to the authors

Table 2. CMIP6 models used in the study

2.3 Evapotranspiration

ArcGIS tools were developed for calculating historical and future average monthly ET_o based on the Penman–Monteith (PM) (Annexure) formula,

$$ET_0 = \frac{.408\Delta(Rn - G) + \gamma \frac{900}{T+273} u_2 (e_s - e_a)}{\Delta + \gamma(1 + .34u_2)} \quad (1)$$

where ET_o is the reference ET_o (mm day^{-1}), Rn is the net radiation at the crop surface (MJ $m^{-2}day^{-1}$), G is the soil heat flux density (MJ m^{-2} day^{-1}), T is the mean air temperature at 2 m height (°C), U_2 is the wind speed at 2 m height (ms^{-1}), e_s is the saturation vapor pressure (kPa), e_a is the actual vapor pressure (kPa), Δ is the slope of vapor pressure curve (kPa $°C^{-1}$) and γ is the psychometric constant (kPa $°C^{-1}$) (Allen *et al.*, 1998).

For historical ET_o, the meteorological data required for calculations are available. However, for future calculations, the actual vapor pressure and solar radiation are unavailable; consequently, a method was used to predict them based on the available historical data.

2.4 Future actual vapor pressure

The actual vapor pressure (ea) is the vapor pressure at the dewpoint temperature (Tdew) [°C] (Allen *et al.*, 1998),

$$e_a = 0.6108 * e^{\left(\frac{17.27T_{dew}}{237.3+T_{dew}}\right)} \quad (2)$$

As historical vapor pressure is available, the historical dewpoint temperature was calculated. Then the ratio between it and the historical minimum temperature was calculated. Future dewpoint temperature was calculated as follows:

$$(T_{dew})_{future} = (T_{min})_{future} * \left(\frac{T_{dew}}{T_{min}}\right)_{historical} \quad (3)$$

They were then followed by calculating future vapor pressure from equation (2) .

2.5 Future solar radiation

The difference between the maximum and minimum air temperature (Tmax – Tmin) can be used in calculating solar radiation (Allen *et al.*, 1998),

$$R_{s=K_{Rs}\sqrt{(Tmax - Tmin)}R_a} \quad (4)$$

Where R_s is solar radiation [MJ m^{-2} day^{-1}], R_a is extraterrestrial radiation [MJ m^{-2} d^{-1}], T_{max} is maximum air temperature [°C], T_{min} is minimum air temperature [°C] and k_{Rs} is adjustment coefficient (0.16 . . . 0.19) [°C−0.5].

Extraterrestrial radiation is a function of latitude, date and time of day (Allen *et al.*, 1998). Therefore, it is constant for the historical and future. Future solar radiation was calculated as:

$$(R_s)_{future} = \frac{\left(\sqrt{(Tmax - Tmin)}\right)_{future}}{\left(\sqrt{(Tmax - Tmin)}\right)_{historical}} (R_s)_{historical} \quad (5)$$

3. Results and discussion

3.1 National scale

The average monthly ET_o was calculated for the historical period (1970–2000) and future periods (2020–2040 and 2040–2060). The future period's calculations were carried out for the six models' data under the four SSP scenarios. Figures 2–10 show the average monthly ET_o for the historical period (1970–2000), the future period (2020–2040) under SSP126, SSP245, SSP370 and SSP585 scenarios, and 2040–2060 under SSP126, SSP245, SSP370 and SSP585 scenarios, respectively. The research findings unveiled that the peak monthly ET_o values were concentrated in the southern region of the country during the summer season. This occurrence can be attributed to the region's elevated temperature levels (FAO, 2016), where air temperature emerges as the foremost influencer of (Liu *et al.*, 2014; Sun *et al.*, 2020) northern part of the country experienced the lowest ET_o values during the winter, which can be attributed to the colder temperatures in this region. This pattern held true for both historical and future periods.

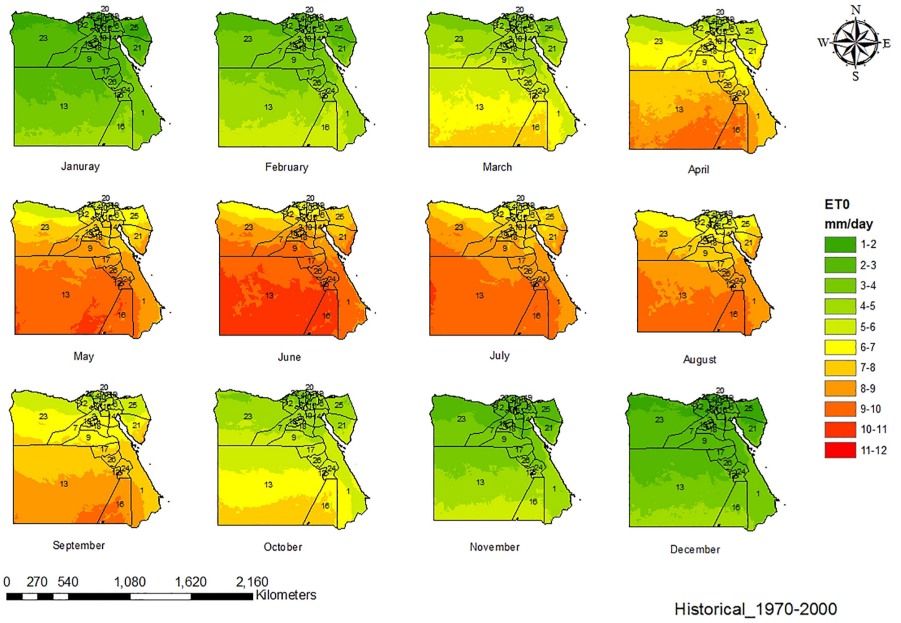

Source(s): Credited to the authors

Figure 2.
Average monthly ET_o (mm/day) for the period (1970–2000)

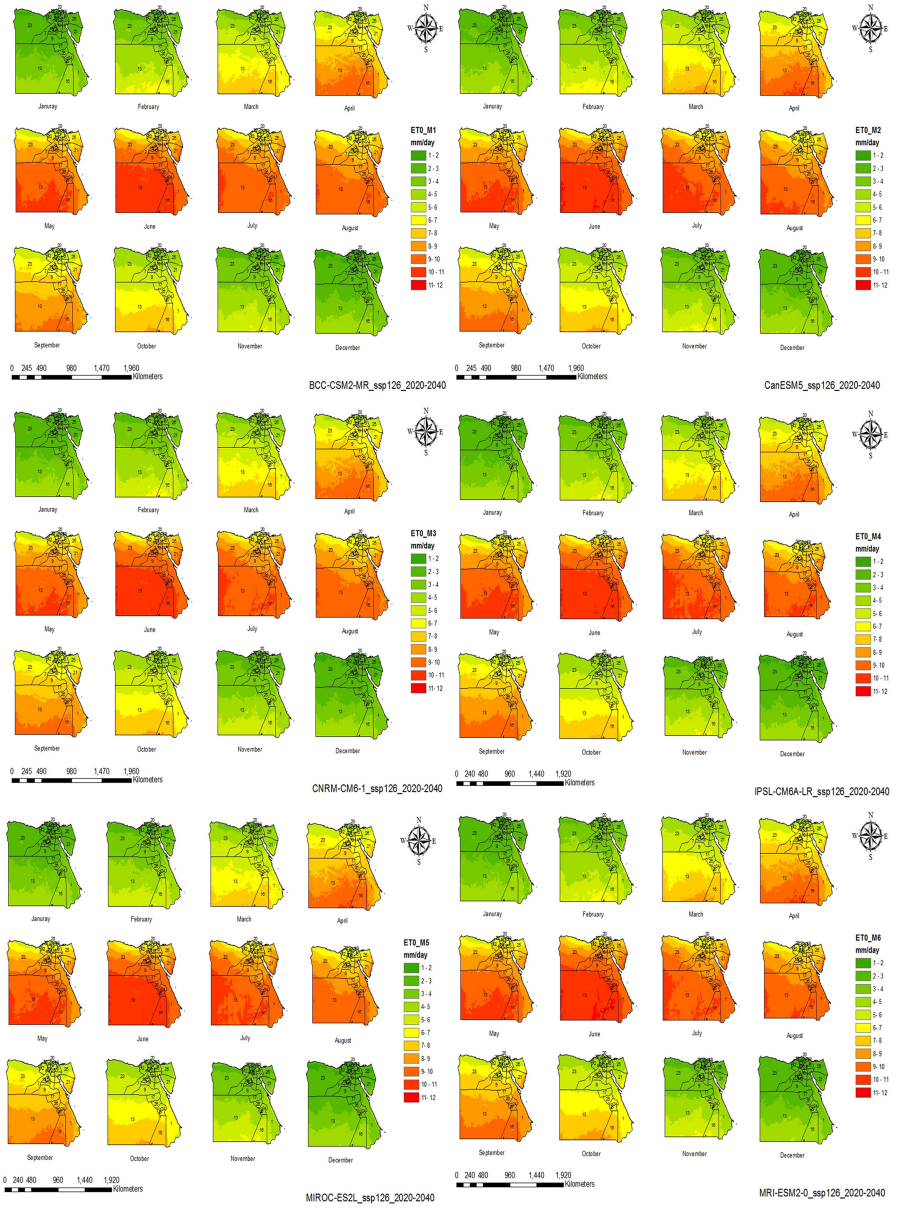

Figure 3.
Average monthly ET_o (mm/day) for the period (2020–2040) under SSP126 for the six models

Source(s): Credited to the authors

3.2 Subnational scale

The average monthly ET_o for Egypt's governorates at the subnational scale was computed for both historical and future periods, encompassing the four SSP scenarios analyzed across six models (Annexure for specific details). This calculation involved averaging the results for each governorate zone and subsequently averaging the outcomes from all six models.

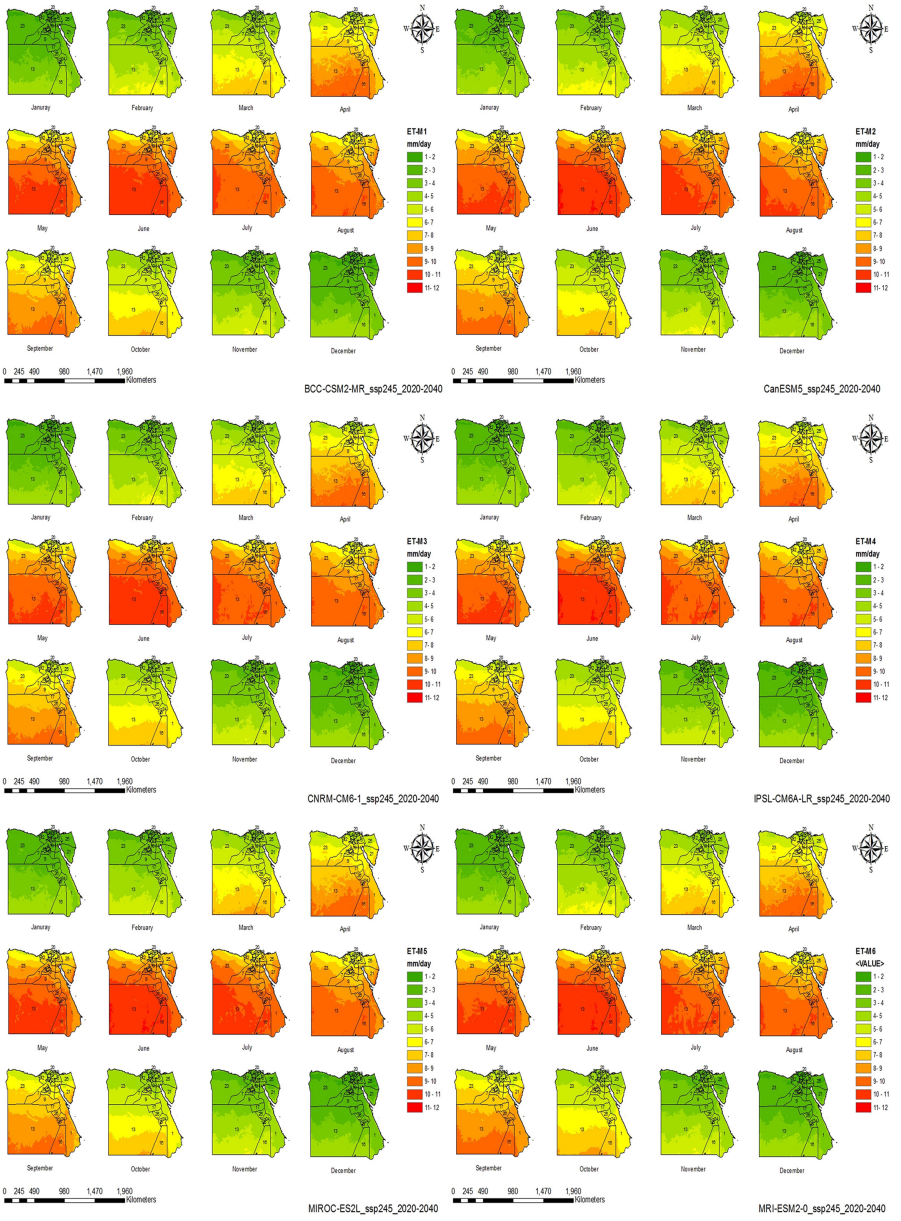

Source(s): Credited to the authors

Figure 4.
Average monthly ET_o (mm/day) for the period (2020–2040) under SSP245 for the six models

Additionally, the average annual ET_o values were ascertained to facilitate data presentation, as illustrated in Figures 11 and 12. To provide a comprehensive view of the data, the percentage difference in ET_o between future and historical calculations is presented in Table 3. Notably, four governorates, namely Al Bahr al Ahmar, Janub Sina', Matrouh and Al

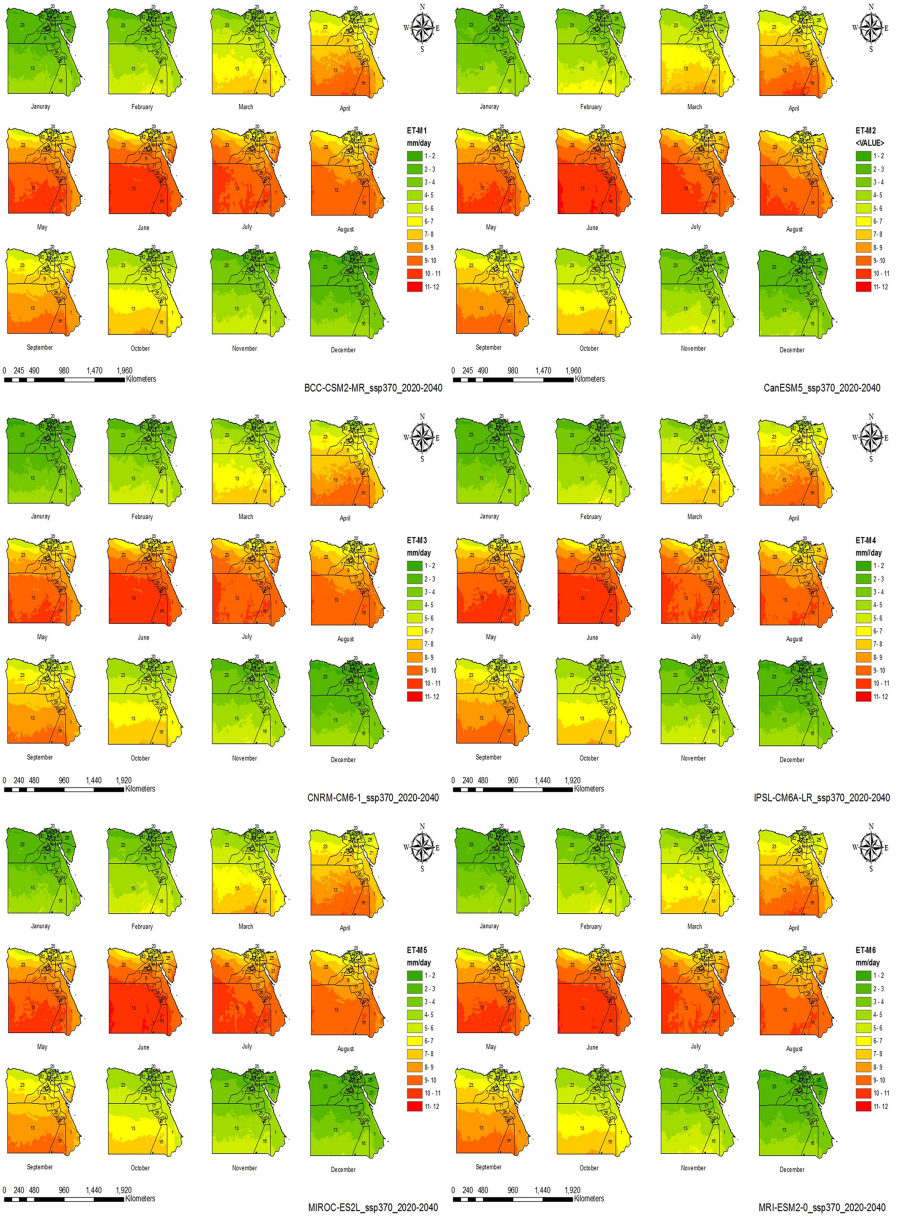

Source(s): Credited to the authors

Figure 5.
Average monthly ET_o (mm/day) for the period (2020–2040) under SSP370 for the six models

Wadi al Jadid, were excluded from the analysis due to their limited agricultural significance (CAPMAS, 2021).

For the near future period (2020–2040), the calculation illustrated increasing values compared to the historical period (1970–2000), showing minimal fluctuations across the four

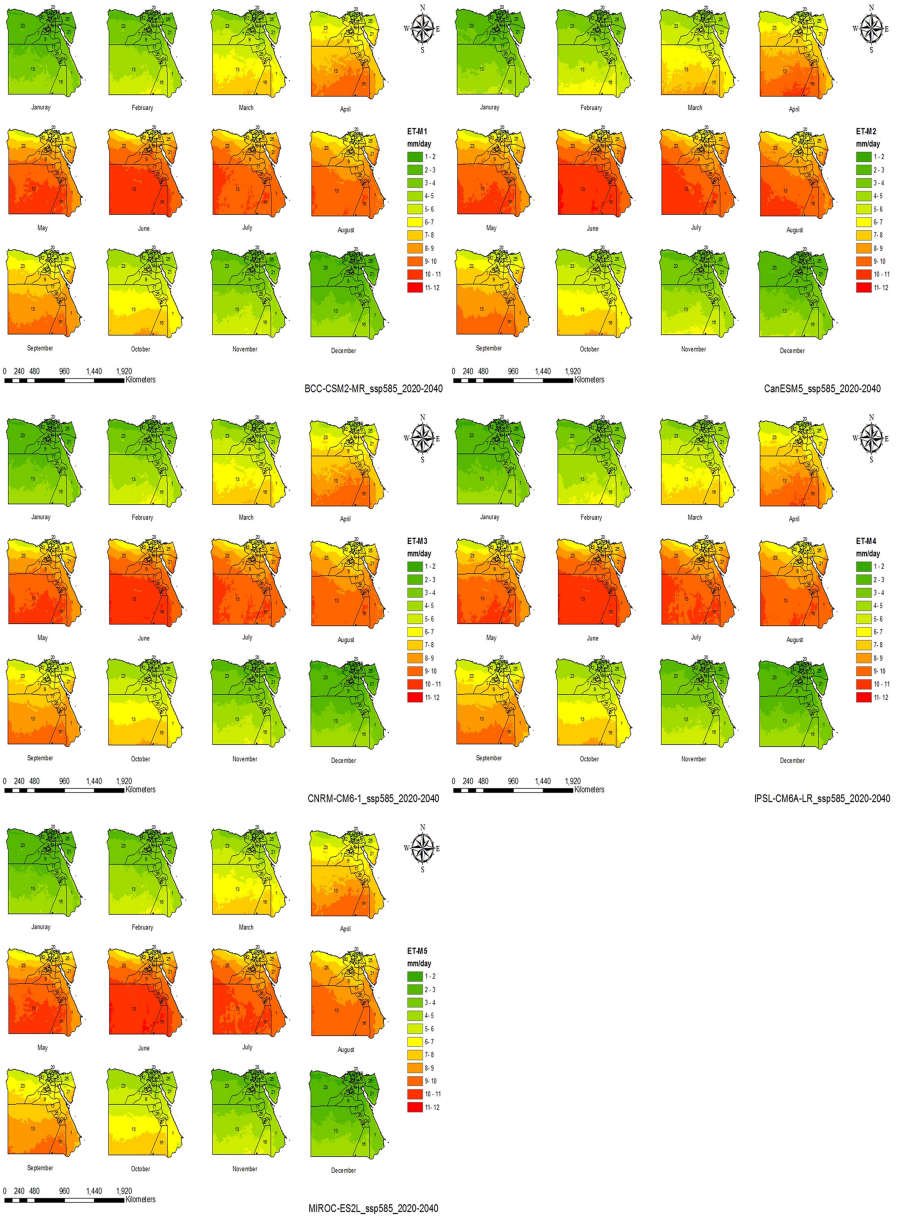

Source(s): Credited to the authors

Figure 6.
Average monthly ET_o (mm/day) for the period (2020–2040) under SSP585 for the six models

climatic scenarios. This can be attributed to the escalating temperatures resulting from climate change (Das *et al.*, 2022; Liu *et al.*, 2020). Figure 10 shows the highest average annual ET_o value equal to 7.82 mm/day at Aswan, while the lowest value equals 4.21 mm/day at Kafr ash Shaykh. This disparity can be ascribed to these respective governorates' notably high and low

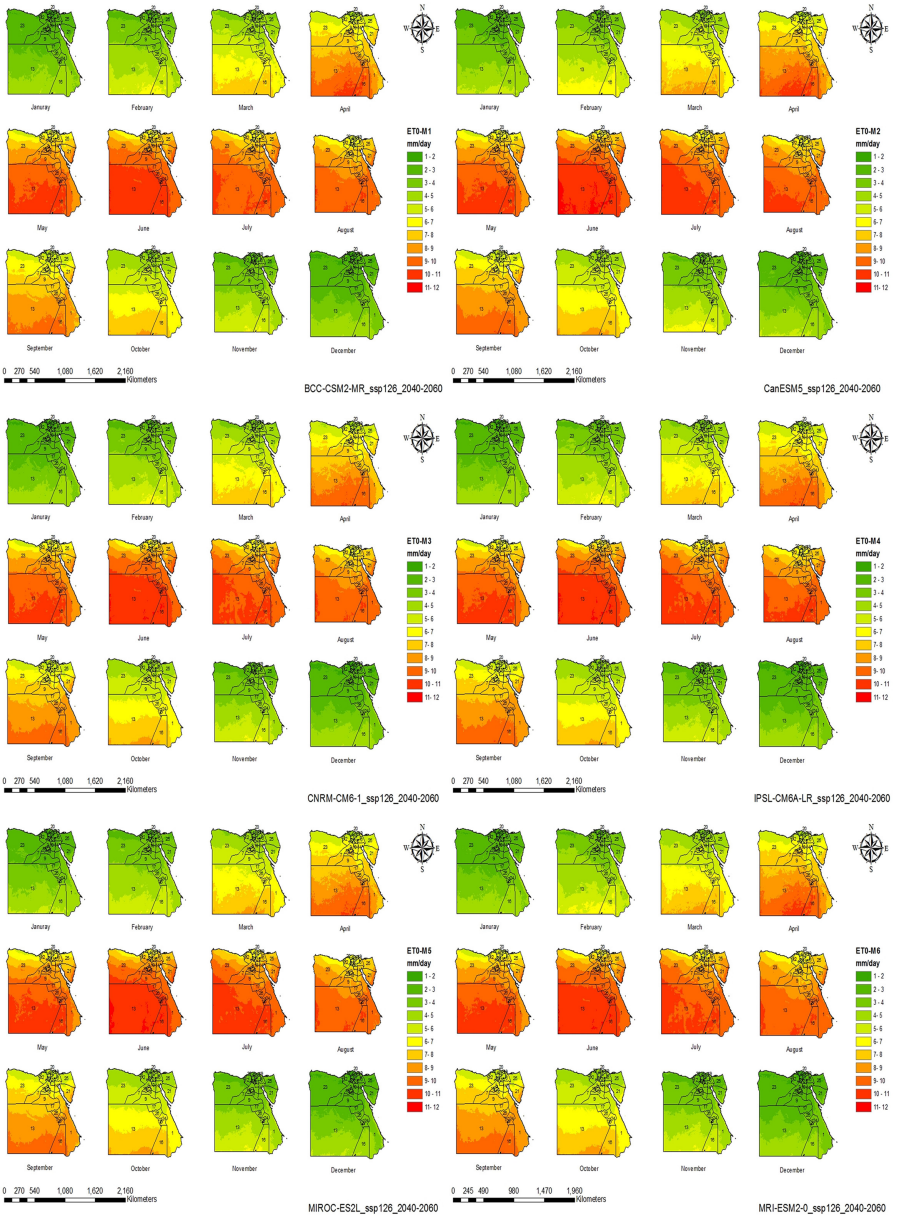

Figure 7.
Average monthly ET_o (mm/day) for the period (2040–2060) under SSP126 for the six models

Source(s): Credited to the authors

temperatures. For the period (2040–2060), the calculations reveal a significant increase in average annual ET_o compared to the historical period, with substantial differences among the various climate scenarios. The highest average annual ET_o was found at Aswan, with a value of 8.08 mm/day, while the lowest value was at Kafr ash Shaykh, with a value of 4.28 mm/day.

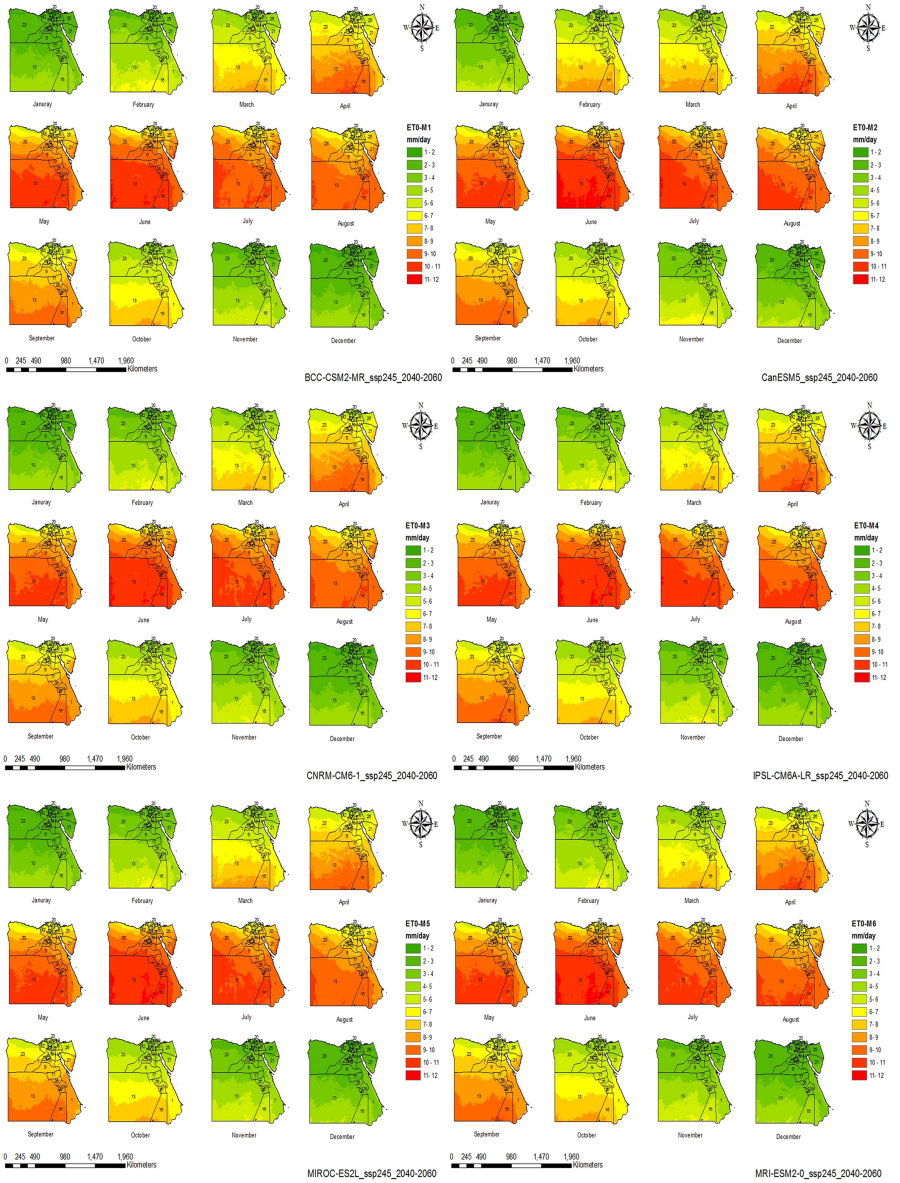

Source(s): Credited to the authors

Figure 8.
Average monthly ET_o (mm/day) for the period (2040–2060) under SSP245 for the six models

Therefore, this clarifies the positive sensitivity of evapotranspiration change to the mean air temperature, which is the first key factor in ET_o change (Liu *et al.*, 2014).

On the other hand, the study results show that the highest difference percentage between future and historical ET_o values are found under the SSP585 scenario for the period of 2040–2060 (Table 3). The highest difference percentage of 12.17% is observed at Shamal Sina'

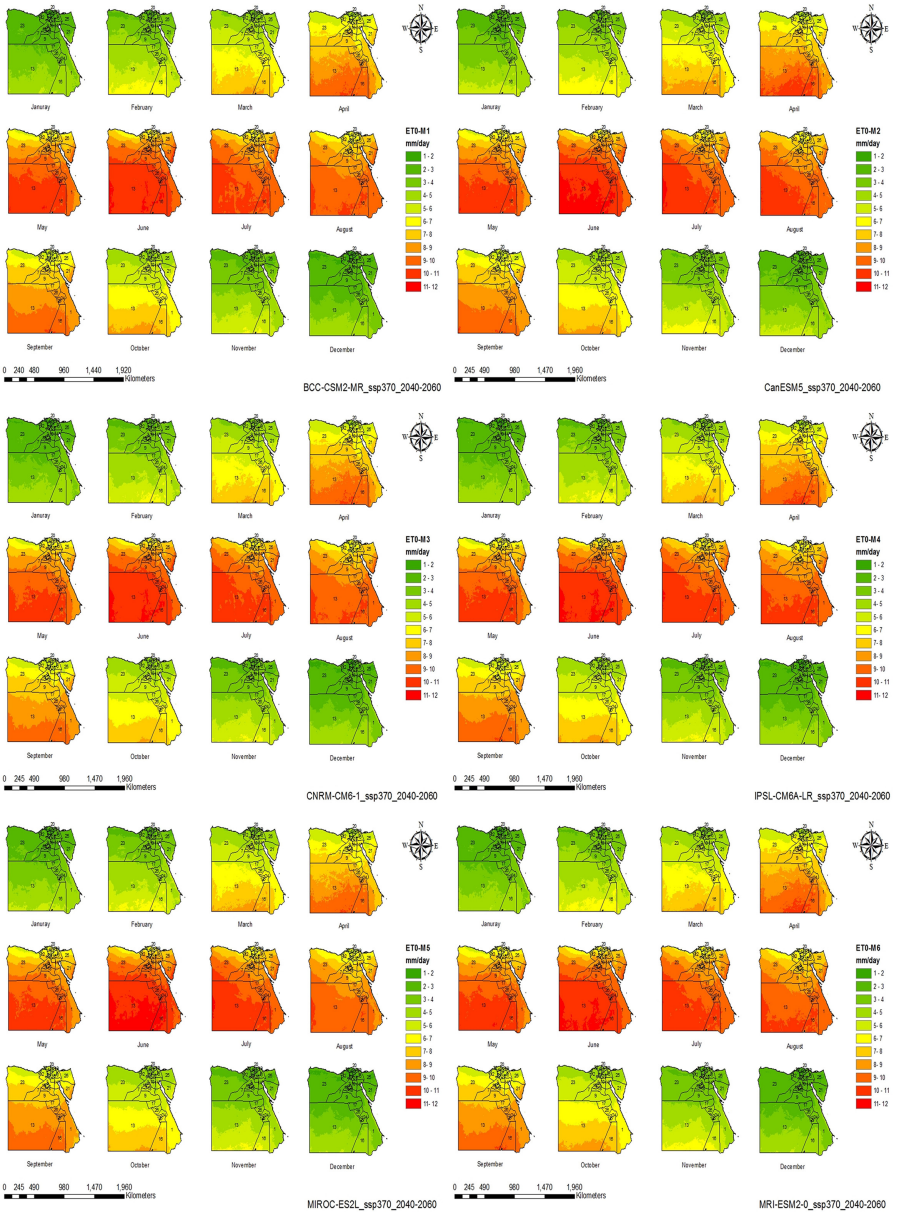

Figure 9.
Average monthly ET_o (mm/day) for the period (2040–2060) under SSP370 for the six models

Source(s): Credited to the authors

under the SSP585 scenario, in contrast, the lowest difference percentage of 4.71% is found at Aswan under the SSP370 scenario. It is worth noting that these results indicate that the northern coastal areas are more vulnerable to climate change as the highest ET_o difference percentage values were found in the coastal region, which is different from previous studies that showed the highest values are in the south (Abdrabbo *et al.*, 2015; Farag *et al.*, 2014).

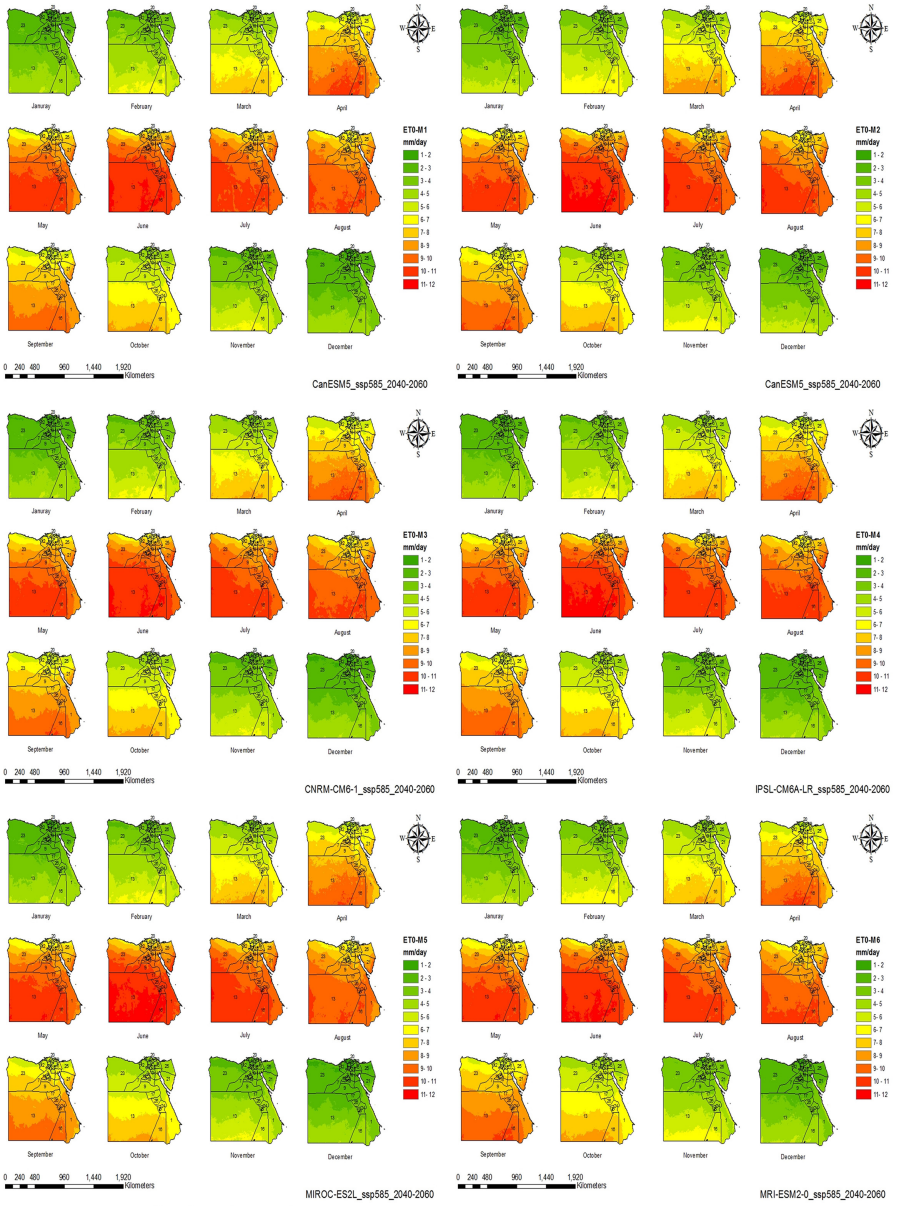

Source(s): Credited to the authors

Figure 10.
Average monthly ET_o (mm/day) for the period (2040–2060) under SSP585 for the six models

This result matches the previous study (Yassen, Nam, & Hong, 2020), which found that the trend of ET_o between (1983 and 2017) in the southeastern and northwestern regions is the most affected by climate change. Nevertheless, there exists a discrepancy in the outcomes compared to the findings of (Farag *et al.*, 2014). This divergence can be attributed to their

omission of accounting for alterations in actual vapor pressure and solar radiation resulting from climate change. Instead, they utilized their existing data, an aspect underscored as influential by Liu *et al.* (2020). This variance may also be attributed to the elevated humidity levels prevalent in the northern regions, as expounded upon by (FAO, 2016).

Given that ET_o is negatively responsive to relative humidity, as highlighted by (Zhang *et al.*, 2019), this difference in humidity could further contribute to the observed distinction in results. These study outcomes are important for policymakers and researchers as they provide valuable insights into understanding the vulnerability of Egypt's irrigation water requirement to climate change. Finally, we noticed that ET_o values are lower under the SSP scenarios than old ones (A1, B1, A2, B2 and RCP 2.6, 4.5, 6, 8.5), which were used in previous studies (Abdrabbo *et al.*, 2015; Farag *et al.*, 2014).

4. Conclusion

In summary, this study underscores the profound influence of climate change on ET_o within Egypt's governorates. This study outcomes reveals pivotal insights by scrutinizing the periods of 2020–2040 and 2040–2060 alongside the historical interval of 1970–2000. Specifically, it unveils the concentration of the highest ET_o values within the southern realm of the country while accentuating the heightened susceptibility of the northern coastal regions to climate shifts. Remarkably, this study unveils a notable contrast to prior findings by pinpointing the coastal region as having the highest percentage disparity in ET_o values,

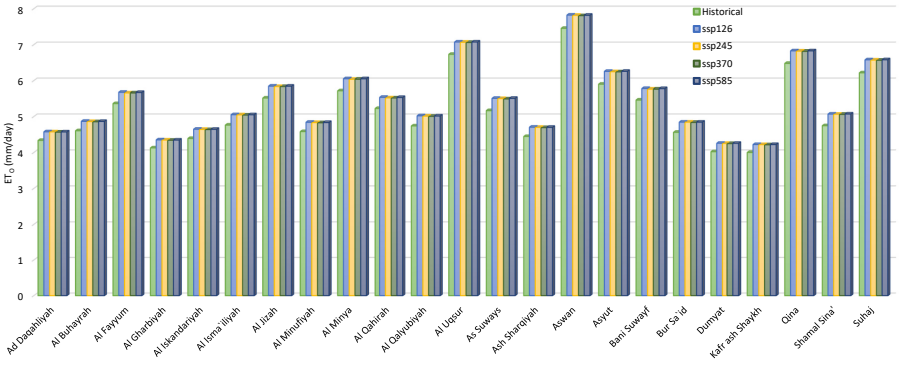

Figure 11.
Average annual ET_o (mm/day) for the period (2020–2040) under the four SSP scenarios and the historical period (1970–2000) for Egypt's governorates

Source(s): Credited to the authors

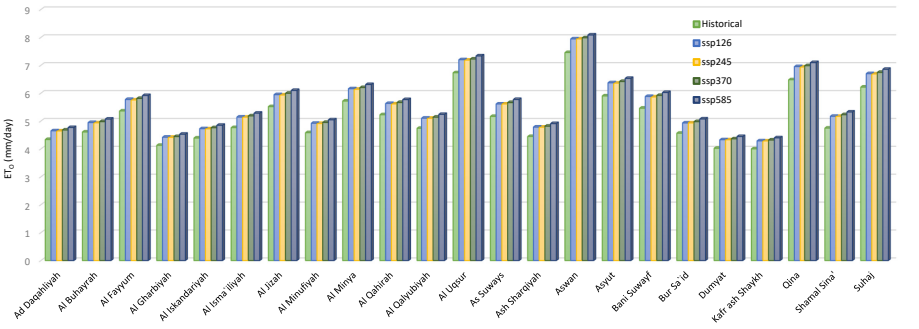

Figure 12.
Average annual ET_o (mm/day) for the period (2040–2060) under the four SSP scenarios and the historical period (1970–2000) for Egypt's governorates

Source(s): Credited to the authors

Gov. Name	2020–2040 SSP126	SSP245	SSP370	SSP585	2040–2060 SSP126	SSP245	SSP370	SSP585
Ad Daqahliyah	5.50	5.48	5.32	5.42	7.18	7.07	7.85	9.88
Al Buhayrah	5.66	5.5	5.40	5.57	7.36	7.15	8.07	10.03
Al Fayyum	5.89	5.53	5.53	5.78	7.69	7.34	8.39	10.31
Al Gharbiyah	5.40	5.29	5.16	5.27	7.02	6.92	7.59	9.62
Al Iskandariyah	5.85	5.73	5.61	5.78	7.60	7.49	8.38	10.39
Al Isma`iliyah	6.04	5.99	5.85	6.00	7.93	7.86	8.81	10.86
Al Jizah	5.99	5.79	5.78	5.96	7.78	7.58	8.66	10.51
Al Minufiyah	5.67	5.48	5.35	5.52	7.36	7.19	8.01	10.04
Al Minya	5.88	5.59	5.65	5.87	7.71	7.38	8.47	10.33
Al Qahirah	5.92	5.62	5.58	5.82	7.71	7.45	8.42	10.40
Al Qalyubiyah	5.92	5.73	5.58	5.77	7.62	7.56	8.39	10.46
Al Uqsur	5.07	5.00	4.89	5.08	6.93	6.70	7.31	8.96
As Suways	6.60	6.49	6.29	6.59	8.63	8.63	9.60	11.75
Ash Sharqiyah	5.83	5.73	5.57	5.71	7.58	7.52	8.32	10.41
Aswan	4.93	4.84	4.71	4.86	6.59	6.58	7.08	8.47
Asyut	6.03	5.86	5.81	6.05	7.97	7.76	8.76	10.65
Bani Suwayf	5.88	5.55	5.56	5.83	7.70	7.39	8.39	10.30
Bur Sa`id	6.21	6.19	6.04	6.18	8.08	8.10	9.07	11.18
Dumyat	5.85	5.77	5.65	5.80	7.61	7.58	8.42	10.49
Kafr ash Shaykh	5.53	5.47	5.34	5.52	7.17	7.09	7.93	9.89
Qina	5.38	5.28	5.18	5.38	7.29	7.09	7.77	9.49
Shamal Sina'	6.82	6.73	6.67	6.86	8.95	8.90	10.13	12.17

Source(s): Credited to the authors

Table 3. ETo difference percentage (%) between future and historical calculations

contrary to the prevailing notion that these differences emanate from the southern territories. Furthermore, the investigation illustrates that during the 2040–2060 period, ET_o values attain their pinnacle across all climate change scenarios, underlining the evolving dynamics. Intriguingly, more recent scenarios predict diminished ET_o values compared to preceding ones (A1, B1, A2, B2 and RCP 2.6, 4.5, 6, 8.5). Conclusively, these findings have significant implications for policymakers and future research endeavors, providing a valuable resource to inform decision-making and guide further investigations. Notably, Egyptian policymakers should prioritize addressing the growing vulnerability of the northern coastal regions to climate shifts by implementing adaptive measures for water resource security. Furthermore, evaluating reduced ET_o values in recent scenarios is crucial for effective water resource management and sustainable agriculture. Additionally, adopting integrated climate resilience strategies, including enhancing water use efficiency, promoting drought-resistant crops and investing in climate-resilient infrastructure, is paramount to successfully adapting to evolving climatic conditions. These measures are essential for safeguarding Egypt's water resources and ensuring the sustainability of its agricultural sector in the context of climate change.

References

Abdrabbo, M., Farag, A., & El-Desokey, W. (2015). Implementing of RCPs scenarios for the prediction of evapotranspiration in Egypt. *International Journal of Plant & Soil Science*, *6*(1), 50–63. doi: 10.9734/ijpss/2015/12721.

Affairs, M. F. F. (2018). Climate change profile Egypt. In *Ministry of Foreign Affairs of the Netherlands*, (July). Available from: www.government.nl/foreign-policy-evaluations

Allen, Pereira, L. S., Raes, D., & Smith, M. (1998). FAO irrigation and drainage paper No. 56, crop evapotranspiration. *Irrigation and Drainage*, *300*(56), 300. doi: 10.1016/j.eja.2010.12.001.

Arunrat, N., Pumijumnong, N., Sereenonchai, S., Chareonwong, U., & Wang, C. (2020). Assessment of climate change impact on rice yield and water footprint of large-scale and individual farming in Thailand. *Science of the Total Environment*, *726*, 137864. doi: 10.1016/j.scitotenv.2020.137864.

Arunrat, N., Sereenonchai, S., Chaowiwat, W., & Wang, C. (2022). Climate change impact on major crop yield and water footprint under CMIP6 climate projections in repeated drought and flood areas in Thailand. *Science of the Total Environment*, *807*, 150741. doi: 10.1016/j.scitotenv.2021.150741.

Bao, Z., Zhang, J., Liu, J., Wang, G., Yan, X., Wang, X., & Zhang, L. (2012). Sensitivity of hydrological variables to climate change in the Haihe River basin, China. *Hydrological Processes*, *26*(15), 2294–2306. doi: 10.1002/hyp.8348.

Boucher, O., Servonnat, J., Albright, A. L., Aumont, O., Balkanski, Y., Bastrikov, V., … Vuichard, N. (2020). Presentation and evaluation of the IPSL-CM6A-LR climate model. *Journal of Advances in Modeling Earth Systems*, *12*(7), 1–52. doi: 10.1029/2019MS002010.

CAPMAS (2021). Central agency for public mobilization and statistics. Available from: https://doi.org/geoportal.capmas.gov.eg

Cardona, O. D., Van Aalst, M. K., Birkmann, J., Fordham, M., Mc Gregor, G., Rosa, P., … Thomalla, F. (2012). Determinants of risk: Exposure and vulnerability. In: *Managing the Risks of Extreme Events and Disasters to Advance Climate Change Adaptation*, [Field, C.B., V. Barros, T.F. Stocker, D. Qin, D.J. Dokken, K.L. Ebi, M.D. Mastrandrea, K.J. Mach, G.-K. Plattner. A Special Report of Working Groups I and II of the Intergovernmental Panel on Climate Change (IPCC). Cambridge University Press, Cambridge, UK, and New York, NY, USA, *65*, 65-108, 9781107025, 65–108. doi: 10.1017/CBO9781139177245.005.

Das, S., Datta, P., Sharma, D., & Goswami, K. (2022). Trends in temperature, precipitation, potential evapotranspiration, and water availability across the teesta river basin under 1.5 and 2 ℃ temperature rise scenarios of CMIP6. *Atmosphere*, *13*(6), 1–22. doi: 10.3390/atmos13060941.

El Afandi, G., & Abdrabbo, M. (2015). Evaluation of reference evapotranspiration equations under current climate conditions of Egypt. *Turkish Journal of Agriculture - Food Science and Technology*, *3*(10), 819. doi: 10.24925/turjaf.v3i10.819-825.481.

FAO (2016). Country profile - Egypt - aquatstat. Available from: https://www.fao.org/aquastat/en/countries-and-basins/country-profiles/country/PRT

Farag, A. A., Abdrabbo, M. A. A., & Ahmed, M. S. M. (2014). GIS tool for distribution reference evapotranspiration under climate change in Egypt. *International Journal of Plant & Soil Science*, *3*(6), 575–588. doi: 10.9734/ijpss/2014/8172.

Fick, S. E., & Hijmans, R. J. (2017). WorldClim 2: New 1-km spatial resolution climate surfaces for global land areas. *International Journal of Climatology*, *37*(12), 4302–4315. doi: 10.1002/joc.5086.

Giorgi, F. (2006). Climate change hot-spots. *Geophysical Research Letters*, *33*(8), 1–4. doi: 10.1029/2006GL025734.

Good, S. P., Noone, D., & Bowen, G. (2015). Hydrologic connectivity constrains partitioning of global terrestrial water fluxes. *Science*, *349*(6244), 175–177. doi: 10.1126/science.aaa5931.

Gurara, M. A., Jilo, N. B., & Tolche, A. D. (2021). Impact of climate change on potential evapotranspiration and crop water requirement in Upper Wabe Bridge watershed, Wabe Shebele River Basin, Ethiopia. *Journal of African Earth Sciences*, *180*(April), 104223. doi: 10.1016/j.jafrearsci.2021.104223.

Hajima, T., Watanabe, M., Yamamoto, A., Tatebe, H., Noguchi, M. A., Abe, M., … Kawamiya, M. (2020). Development of the MIROC-ES2L Earth system model and the evaluation of biogeochemical processes and feedbacks. *Geoscientific Model Development*, *13*(5), 2197–2244. doi: 10.5194/gmd-13-2197-2020.

Hamed, M. M., & Shahid, S. (2022). Inter-comparison of historical simulation and future projections of rainfall and temperature by CMIP5 and CMIP6 GCMs over Egypt. October, 2021, 4316–4332. doi: 10.1002/joc.7468.

IPCC (1992). Climate change 1992 the supplementary report to the IPCC scientific assessment. *Intergovernmental Panel on Climate Change*, *220*.

IPCC (2014). Climate change 2014 synthesis report: Summary chapter for policymakers. *Intergovernmental Panel on Climate Change*, *31*. doi: 10.1017/CBO9781107415324.

Liu, H., Zhang, R., & Li, Y. (2014). Sensitivity analysis of reference evapotranspiration (ETo) to climate change in Beijing, China. *Desalination and Water Treatment*, *52*(13-15), 2799–2804. doi: 10.1080/19443994.2013.862030.

Liu, X., Li, C., Zhao, T., & Han, L. (2020). Future changes of global potential evapotranspiration simulated from CMIP5 to CMIP6 models. *Atmospheric and Oceanic Science Letters*, *13*(6), 568–575. doi:10.1080/16742834.2020.1824983.

Meinshausen, M., Nicholls, Z., Lewis, J., Gidden, M., Vogel, E., Freund, M., … Wang, H. J. (2020). The SSP greenhouse gas concentrations and their extensions to 2500. *Geoscientific Model Development*, *13*, 3571–3605. doi: 10.5194/gmd-13-3571-2020.

Moss, R., Babiker, M., Brinkman, S., Calvo, E., Carter, T., Edmonds, J., … Zurek, M. (2008). Towards new scenarios for analysis of emissions, climate change, impacts, and response strategies: IPCC expert meeting report: 19-21 september, 2007, noordwijkerhout, The Netherlands. In *Intergovernmental Panel on Climate Change*. Geneva.

Moss, R., Edmonds, J. A., Hibbard, K. A., Manning, M. R., Rose, S. K., Van Vuuren, D. P., … Wilbanks, T. J. (2010). The next generation of scenarios for climate change research and assessment. *Nature*, *463*(7282), 747–756. doi: 10.1038/nature08823.

MWRI (2014). Water scarcity in Egypt: The urgent need for regional cooperation among the nile basin countries. *Ministry of Water Resources and Irrigation, Water Scaricity*, 1–5.

Nashwan, M. S., & Shahid, S. (2022). Future precipitation changes in Egypt under the 1.5 and 2.0 °C global warming goals using CMIP6 multimodel ensemble.pdf. *Atmospheric Research*, *265*, 105908. doi: 10.1016/j.atmosres.2021.105908.

Riahi, K., van Vuuren, D. P., Kriegler, E., Edmonds, J., O'Neill, B. C., Fujimori, S., … Tavoni, M. (2017). The Shared Socioeconomic Pathways and their energy, land use, and greenhouse gas emissions implications: An overview. *Global Environmental Change*, *42*, 153–168. doi: 10.1016/j.gloenvcha.2016.05.009.

Rim, C. S. (2009). The effects of urbanization, geographical and topographical conditions on reference evapotranspiration. *Climatic Change*, *97*(3), 483–514. doi: 10.1007/s10584-009-9618-y.

Sector, P. (2005). National water resource plan 2017.

Sun, J., Wang, G., Sun, X., Lin, S., Hu, Z., & Huang, K. (2020). Elevation-dependent changes in reference evapotranspiration due to climate change. *Hydrological Processes*, *April*, 1–15. doi: 10.1002/hyp.13978.

Swart, N. C., Cole, J. N. S., Kharin, V. V., Lazare, M., Scinocca, J. F., Gillett, N. P., … Winter, B. (2019). The Canadian earth system model version 5 (CanESM5.0.3). *Geoscientific Model Development*, *12*(11), 4823–4873. doi: 10.5194/gmd-12-4823-2019.

Tadese, M., Kumar, L., & Koech, R. (2020). Long-term variability in potential evapotranspiration, water availability and drought under climate change scenarios in the Awash River Basin, Ethiopia. *Atmosphere*, *11*(9). doi: 10.3390/ATMOS11090883.

Voldoire, A., Saint-Martin, D., Sénési, S., Decharme, B., Alias, A., Chevallier, M., … Waldman, R. (2019). Evaluation of CMIP6 DECK experiments with CNRM-CM6-1. *Journal of Advances in Modeling Earth Systems*, *11*(7), 2177–2213. doi: 10.1029/2019MS001683.

Wu, T., Lu, Y., Fang, Y., Xin, X., Li, L., Li, W., … Liu, X. (2019). The Beijing Climate center climate system model (BCC-CSM): The main progress from CMIP5 to CMIP6. *Geoscientific Model Development*, *12*(4), 1573–1600. doi: 10.5194/gmd-12-1573-2019.

Yassen, A. N., Nam, W. H., & Hong, E. M. (2020). Impact of climate change on reference evapotranspiration in Egypt. *Catena*, *194*(April 2019), 104711. doi: 10.1016/j.catena.2020.104711.

Yukimoto, S., Kawai, H., Koshiro, T., Oshima, N., Yoshida, K., Urakawa, S., ... Ishii, M. (2019). The meteorological research institute Earth system model version 2.0, MRI-ESM2.0: Description and basic evaluation of the physical component. *Journal of the Meteorological Society of Japan*, *97*(5), 931–965. doi: 10.2151/jmsj.2019-051.

Zakaria, S., Al-Ansari, N., & Knutsson, S. (2013). Historical and future climatic change scenarios for temperature and rainfall for Iraq. *Journal of Civil Engineering and Architecture*, *7*(12). doi: 10.17265/1934-7359/2013.12.012.

Zhang, T., Chen, Y., & Paw, U. K. T. (2019). Quantifying the impact of climate variables on reference evapotranspiration in Pearl River Basin, China. *Hydrological Sciences Journal*, *64*(16), 1944–1956. doi: 10.1080/02626667.2019.1662021.

Zhao, Z., Wang, H., Wang, C., Li, W., Chen, H., & Gong, S. (2020). Impacts of climatic change on reference crop evapotranspiration across different climatic zones of Ningxia at multi-time scales from 1957 to 2018. *Advances in Meteorology*, *2020*(56). doi: 10.1155/2020/3156460.

Annexure

The supplementary material for this article can be found online.

Corresponding author

Abdelhamid Ads can be contacted at: abdelhamedads@gmail.com